

# Patterns of neonatal hypoxic–ischaemic brain injury

Linda S. de Vries · Floris Groenendaal

Received: 18 February 2010 / Accepted: 26 February 2010 / Published online: 14 April 2010  
© The Author(s) 2010. This article is published with open access at Springerlink.com

**Abstract** Enormous progress has been made in assessing the neonatal brain, using magnetic resonance imaging (MRI). In this review, we will describe the use of MRI and proton magnetic resonance spectroscopy in detecting different patterns of brain injury in (full-term) human neonates following hypoxic–ischaemic brain injury and indicate the relevance of these findings in predicting neurodevelopmental outcome.

**Keywords** MRI · MRS · Neonatal neuroimaging–perinatal asphyxia · Neonate

## Introduction

Fifty years ago, experiments have demonstrated that perinatal asphyxia could induce brain injury in primates [1]. Since then, different patterns of brain injury have been established [2], which were dependent on the severity and duration of the hypoxic–ischaemic insult. These findings in animal studies were comparable to postmortem findings in asphyxiated human neonates.

During the 1960s to 1980s, imaging of brain injury was performed in human neonates using positron emission

tomography scans and ultrasound. Since the introduction of magnetic resonance imaging (MRI), the knowledge of localisation and severity of brain injury following perinatal asphyxia (hypoxic–ischaemic brain lesions) in surviving neonates has expanded tremendously [3–5]. Diffusion-weighted MRI has enabled us to diagnose lesions much earlier than conventional MRI. MRI can reliably predict neurodevelopmental outcome and may serve as an early biomarker. In addition, phosphorus and proton MR spectroscopy (MRS) have enabled us to detect metabolic changes in the neonatal brain following hypoxia–ischaemia [6, 7]. In this review, we will describe the use of MRI and proton MRS in detecting different patterns of brain injury in (full-term) human neonates following hypoxic–ischaemic brain injury and indicate the relevance of these findings in predicting neurodevelopmental outcome.

## MRI

Although cranial ultrasound can still play a role in the full-term infant with hypoxic–ischaemic brain injury [8], MRI is the method of choice to obtain more detailed and accurate information [5]. The American Academy of Neurology recommended in 2002 that a computed tomography (CT) should be performed to detect haemorrhagic lesions in encephalopathic term infants and MRI only if findings are inconclusive [9]. We do, however, recommend the use of MRI in all full-term infants who present with neonatal encephalopathy and/or seizures. The use of CT is restricted to infants who present with a large intracranial haemorrhage with a shift of the midline seen on cranial ultrasound. These infants may need neurosurgical intervention and access to a CT may be easier, and associated skull fractures may also be better visualised than with MRI [10, 11].

---

L. S. de Vries · F. Groenendaal  
Department of Neonatology,  
Wilhelmina Children's Hospital, University Medical Centre,  
Utrecht, The Netherlands

L. S. de Vries (✉)  
Department of Neonatology, KE 04.123.1,  
Wilhelmina Children's Hospital, University Medical Centre,  
P.O. Box 85090, 3508 AB Utrecht, The Netherlands  
e-mail: l.s.devries@umcutrecht.nl

## Timing of insult

The increased use of neuroimaging techniques and MRI, in particular, has been a tremendous help in timing of brain injury and recognising patterns of injury [4, 12, 13]. Performing MRI within the first 2 weeks after birth, Cowan et al. [13] were able to show that more than 90% of affected newborns had evidence of perinatally acquired lesions on their MRI, with a very low rate of established antenatal brain injury. The presence of ventricular dilatation, widening of the subarachnoid space and interhemispheric fissure, presence of germinolytic cysts or cystic lesions in the white matter, seen at birth or during the first week, are all suggestive of an antenatal insult or an underlying problem, for instance a metabolic disorder [14]. Performing cranial ultrasound on admission is also of value, as most of these lesions suggestive of an antenatal insult or an underlying problem will be recognised with ultrasound. The presence of increased echogenicity in the white matter on a day 1 ultrasound examination is also strongly suggestive of an antenatal insult as this echogenicity takes time to develop. These findings may be important for genetic counselling as well as for medicolegal issues (Fig. 1).

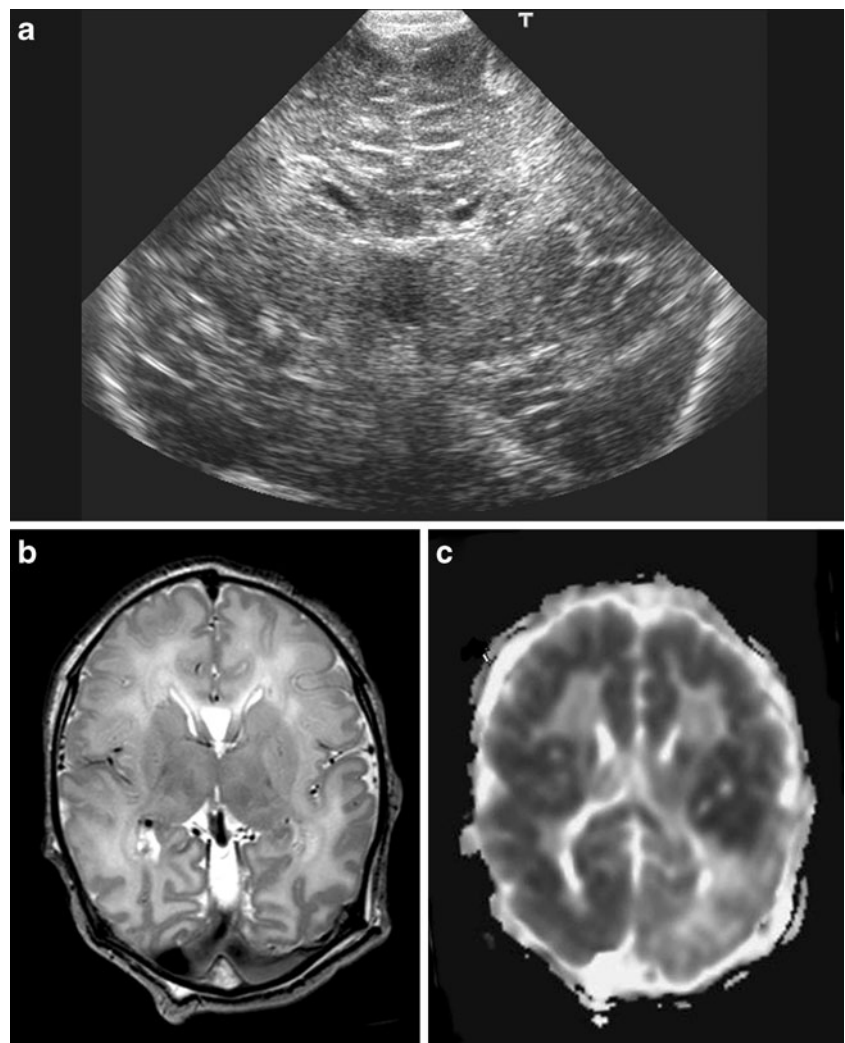
The use of diffusion-weighted imaging (DWI) has also greatly improved our ability to time the onset of brain lesions. A reduced apparent diffusion coefficient can be calculated, showing reduced values (restricted diffusion) during the first few days after the insult, with pseudonormalisation by the end of the first week [15–17]. Sequential imaging has shown that lesions in the basal ganglia may increase in size and site during the first week after birth [18, 19]. Barkovich et al. [19] performed sequential imaging in ten newborn infants and noted that patterns of injury varied considerably during the first 2 weeks after injury. The appearance of new areas of reduced diffusion simultaneous with the pseudonormalisation of areas that had reduced diffusion at earlier times could result in an entirely different pattern of injury on ADC maps acquired at different time points. One therefore needs to be aware of these evolving patterns.

## Main patterns of injury

Comparable to studies in a primate model [2], two main patterns of injury can be distinguished with MRI in the full-term neonate:

1. *Basal ganglia–thalamus pattern (BGT)* predominantly affecting bilaterally the central grey nuclei (ventrolateral thalami and posterior putamina) and perirolandic cortex. Associated involvement of the hippocampus and brain stem is not uncommon (Fig. 2). This pattern of injury is most often seen following an acute sentinel event, for instance a ruptured uterus, placental abruption or a prolapsed cord [3], and is also referred to as a pattern following ‘acute near total asphyxia’ [12, 20]. Using conventional MRI, it was first shown by Rutherford et al. [21] that absence of a normal high-signal intensity of the posterior limb of the internal capsule (PLIC) is highly predictive of severe adverse sequelae. Using conventional MRI, an inversion of the signal within the PLIC is only seen from 48 to 72 h onwards. When MRI is performed early, DWI will already show changes in the basal ganglia/thalami. More accurate information about timing of injury can sometimes be obtained when measuring the apparent diffusion coefficients, but due to evolution over time, this is mainly helpful in the most severely affected infants, who have an MRI performed within the first few days after birth [16, 22]. Hunt et al. [23] measured ADC values within the PLIC in 28 term infants with a clinical diagnosis of hypoxic–ischaemic encephalopathy (HIE) at a mean age of 5.6 days. ADC values were significantly associated with survival and motor outcome. Measuring fractional anisotropy (FA) was noted to be superior to measuring ADC values in predicting outcome [24]. While reduced ADC values were only found in infants with severe encephalopathy, reduced FA values were found in infants with severe and moderate encephalopathy [24]. Children with the BGT pattern of injury tend to be severely disabled due to dyskinetic cerebral palsy (CP). Himmelmann et al. [25] studied 48 children at a mean age of 9 years (range 4–13 years) with dyskinetic CP mostly due to BGT injury and found that most children had Gross Motor Function Classification System levels of level IV,  $n=10$ , and level V,  $n=28$ . The rate of learning disability ( $n=35$ ) and epilepsy ( $n=30$ ) increased with the severity of the motor disability.
2. *Watershed predominant pattern of injury (WS)* is the other pattern of injury which is also referred to as a pattern seen following ‘prolonged partial asphyxia’. The vascular watershed zones (anterior–middle cerebral artery and posterior–middle cerebral artery) are involved, affecting white matter and in more severely affected infants also the overlying cortex (Fig. 3). The lesions can be uni- or bilateral, posterior and/or anterior. Although loss of the cortical ribbon and therefore the grey–white matter differentiation can be seen on conventional MRI, DWI highlights the abnormalities and is especially helpful in making an early diagnosis [26, 27]. A repeat MRI may show cystic evolution, but more often atrophy and gliotic changes will be recognised [28]. It is also more common after hypotension, infection and hypoglycaemia, all of which may be associated with a more protracted course [29]. Neurological manifestations at birth may be

**Fig. 1** Cranial ultrasound, coronal view, day 1, showing severe echogenicity in the white matter. MRI (T<sub>2</sub>SE (TR 6284/TE 120) and ADC) performed on day 3 showing increased signal intensity in the white matter on T<sub>2</sub>SE and low signal intensity in the deep white matter on the ADC map with sparing of the anterior periventricular white matter and asymmetrical distribution in the parieto-occipital white matter. The child died and was subsequently diagnosed to have molybdenum cofactor deficiency

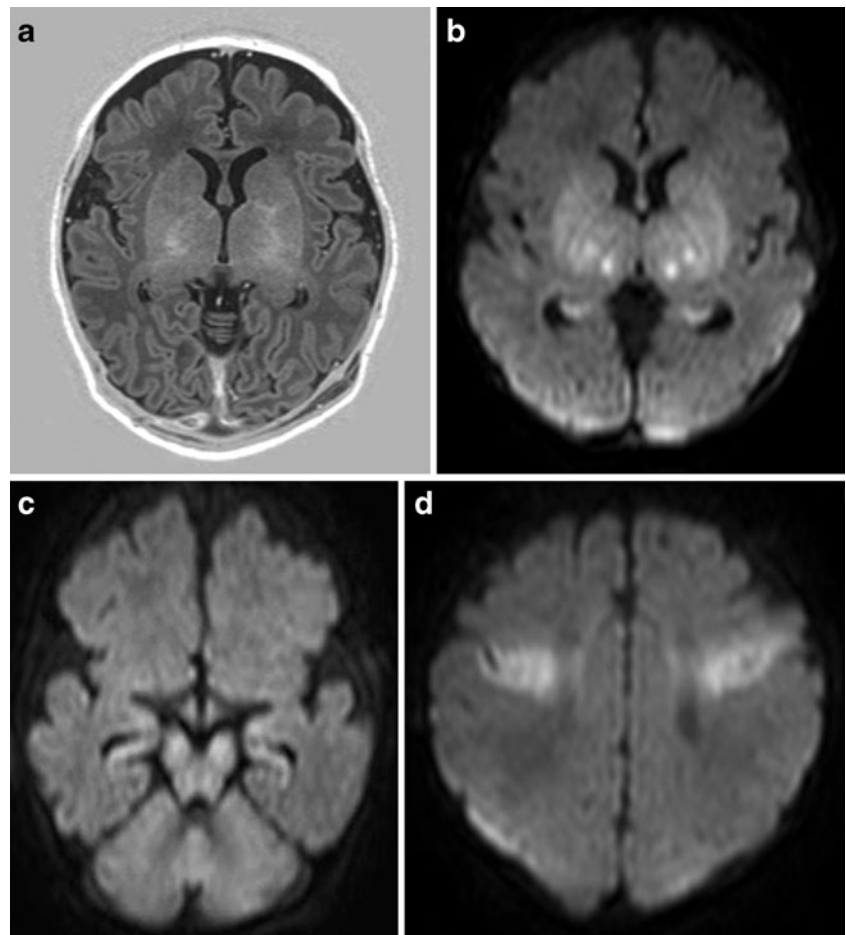


mild and do not always meet the perinatal asphyxia criteria and onset of neurological signs can be delayed [30]. Severe motor impairment is uncommon in this group of infants, and they are often considered to have an early normal outcome, when seen at 12–18 months. When seen up till early childhood suboptimal head growth, behavioural problems and delay in language are, however, common [31, 32]. Miller et al. [33] were first able to recognise cognitive deficits associated with the watershed pattern of injury at 30 months, while the problems were largely overlooked, when seen at 12 months. More recently, they also showed a correlation with verbal IQ at 4 years of age [32]. Symptomatic parieto-occipital epilepsy may occur later in childhood, often associated with reduced intelligence quotients and visuospatial cognitive functions [34].

3. Although not very common, severe involvement of the subcortical white matter and cortex can be seen with relative sparing of the immediate periventricular white matter and central grey matter, referred to as the

‘white cerebrum’, as DWI shows an almost completely white cerebrum, contrasted to a normal looking cerebellum [35] (Fig. 4). This condition tends to be fatal, but in case of survival, multicystic encephalomalacia will develop. An association was recently shown with homozygosity for the 677C>T allele [36]. The prevalence of the 677C>T allele was studied in 11 children with HIE, their respective mothers and 85 healthy individuals. Seven mothers were homozygous and four heterozygous for the 677C>T allele. Five of the children were homozygous and six heterozygous for this polymorphism. The variant allele frequency was higher in the group of mothers with affected children than in the controls and was associated with an increase in plasma homocysteine after methionine loading. The 677C>T mutation in mothers, either in a homozygous or heterozygous state, together with poor nutritional status (probable folate deficiency) may represent a risk factor for irreversible brain injury in the offspring.

**Fig. 2** Full-term infant with acute sentinel event (ruptured uterus) with MRI pattern suggestive of acute near total asphyxia. **a** Inversion recovery sequence (TR 5038/TE 30/TI 600) does not show a normal signal within the posterior limb of the internal capsule, but areas of increased signal intensity within thalami and basal ganglia. DWI (**b–d**) shows restricted diffusion in the ventrolateral thalami, lentiform nuclei, cerebral peduncles, and in the perirolandic cortex. Also note involvement of the hippocampi



4. Another pattern of brain injury consists of “lesions restricted to the periventricular white matter”, not dissimilar from the so-called punctate white matter lesions in the preterm infant (Fig. 5). Li et al. [37] diagnosed this pattern of injury in 23% of their infants and pointed out that infants with this type of injury are significantly less mature with a milder degree of

encephalopathy and fewer clinical seizures relative to other newborns in their cohort, who were diagnosed to have the two more common patterns of injury. This pattern of brain injury is also seen in newborn infants with congenital heart defects [38].

5. *Perinatal arterial ischaemic stroke (PAIS)*, *perinatal haemorrhagic stroke (PHS)* and *sinovenous thrombosis*

**Fig. 3** Full-term infant with watershed pattern of injury. Born with severe anaemia (Hb 2.2 mmol/l) following fetomaternal transfusion and a short period of hypoglycaemia (<1.1 mmol/l). Loss of cortical ribbon is noted on the T<sub>2</sub>SE (TR 6284/TE 120; **a**), and the corpus callosum appears to be swollen with increased signal intensity. **b** The ADC map shows low-signal intensity in the posterior watershed areas, as well as the splenium of the corpus callosum and the optic radiation

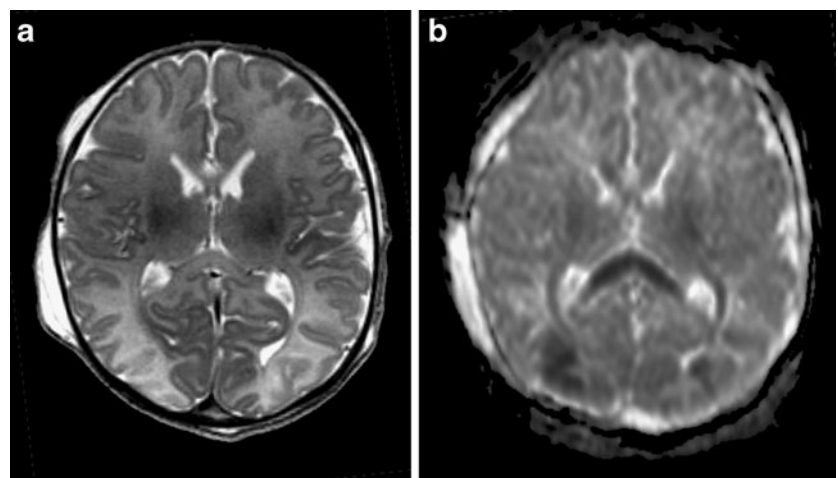
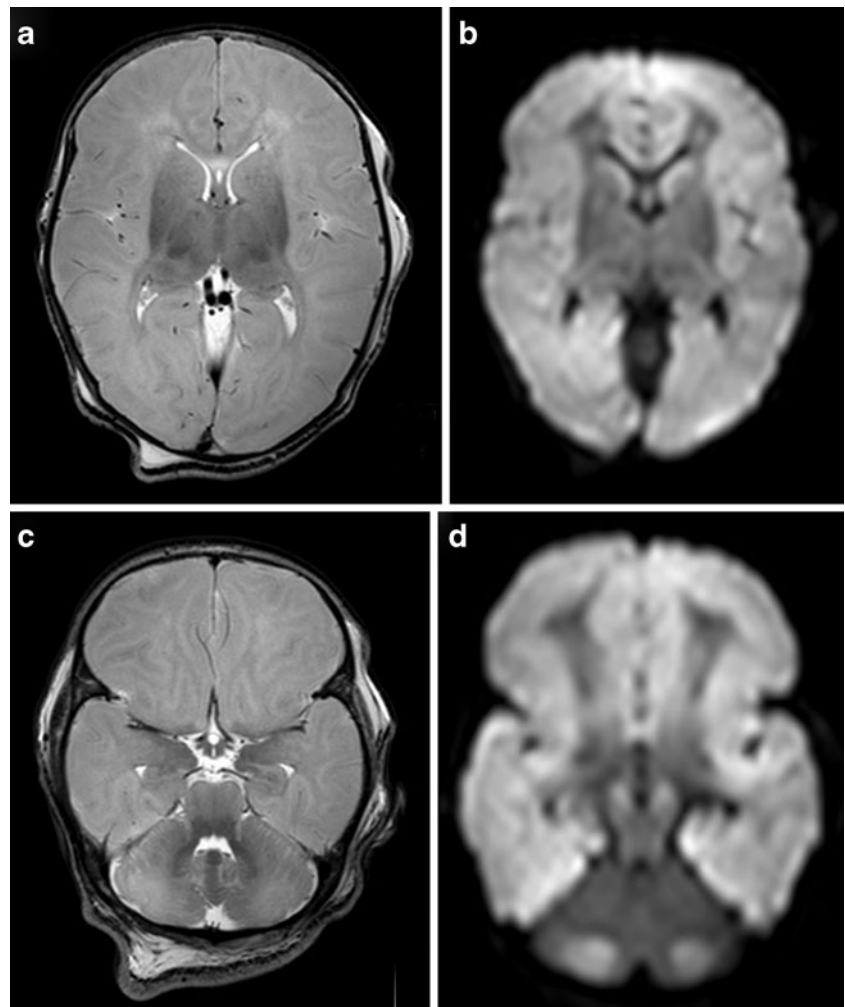




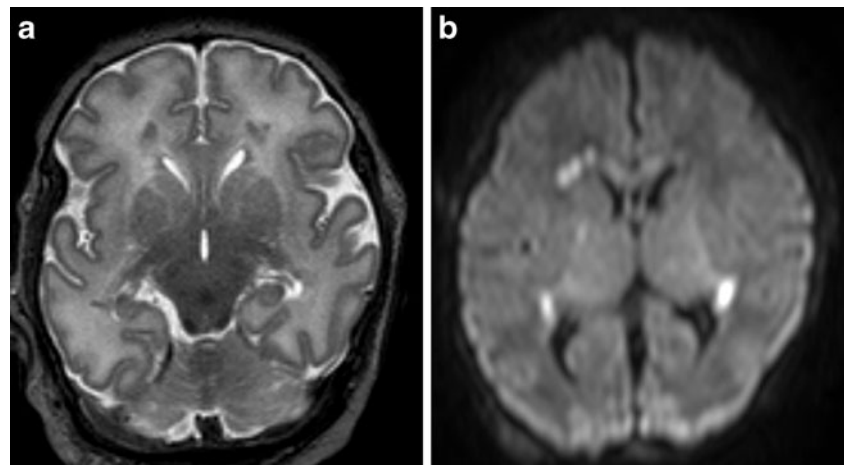
**Fig. 4** Full-term infant with ‘white brain’ pattern of injury. **a, c** T<sub>2</sub>SE (TR 6284/TE 120) shows increased signal intensity in the white matter with loss of cortical ribbon. There is relative sparing of the basal ganglia and immediate periventricular white matter. DWI (**b, d**) confirms the abnormalities and shows a striking discrepancy in signal intensity with the cerebellum. Note high-signal intensity of the mesencephalon (**c**) on T<sub>2</sub>SE and symmetrical restricted diffusion in the cerebral peduncles and also in the cerebellum (**d**)



can also be seen in newborn infants presenting with neonatal encephalopathy and/or seizures. PAIS was found to be related to perinatal asphyxia in only six out of 124 infants [39]. Our own experience and that of others, however, do suggest that the obstetric history is more complicated in infants presenting with PAIS, and

there is often a history of an abnormal cardiocograph, an instrumental delivery or an emergency caesarean section [40]. Cranial ultrasound may be normal if the stroke is superficial and ischaemic, or it may reveal a wedge-shaped area of increased echogenicity with a linear demarcation line, usually within the territory of

**Fig. 5** Full-term infant with punctate white matter lesions seen as low signal intensity changes on T<sub>2</sub>SE (TR 6284/TE 120) and as areas of restricted diffusion on DWI. There is also mild involvement of the corpus callosum and PLIC, seen on DWI



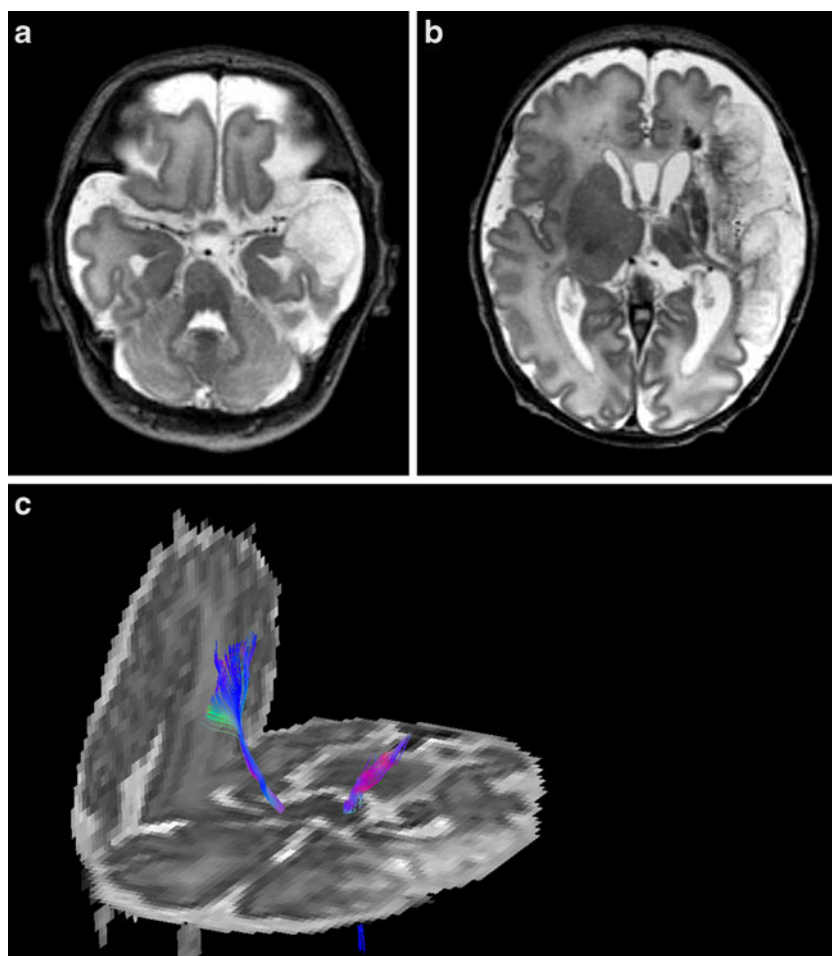
the middle cerebral artery. The echogenicity tends to become visible during the second half of the first week [41]. MRI, including DWI, and MR angiography are by far superior to head ultrasound and should be performed in any newborn presenting with neonatal seizures and especially hemiconvulsions. The role of DWI in the prediction of motor outcome was recently shown [42, 43] with restricted diffusion within the descending corticospinal tracts. Restricted diffusion at the level of the internal capsule and especially the middle part of the cerebral peduncle is now referred to as ‘pre-Wallerian degeneration’ as it is followed by Wallerian degeneration at 6–12 weeks and beyond. Presence of Wallerian degeneration at birth suggests an antenatal onset of the insult (Fig. 6).

Recently developed techniques, such as diffusion tensor imaging (DTI), will allow quantification and visualisation of white matter pathways in vivo [44]. DTI characterises the 3D spatial distribution of water diffusion in each MRI voxel. Water diffuses preferentially along the direction of the axons and is restricted perpendicular to axons by

myelin. This directional dependency is referred to as anisotropy. Directionality encoded colour maps (red–green–blue) or fibre trackings are commonly used. A FA map can show asymmetry of the PLIC as early as the neonatal period. In a study of 15 patients with congenital hemiparesis due to different causes, studied at a median age of 2 years and compared with 17 age-matched controls, clinical severity of hemiparesis was noted to correlate with asymmetry in fractional anisotropy ( $p < 0.0001$ ), transverse diffusivity ( $p < 0.0001$ ) and mean diffusivity ( $p < 0.03$ ) [45]. Another promising technique is volumetric determination of stroke volumes, which was noted to predict motor outcome in animal studies [46]. Functional MRI tends to be used in childhood or adolescence to study reorganisation of the sensorimotor cortex [47, 48], but it was recently shown that passive unilateral sensorimotor stimulation is feasible even in the preterm infant resulting in bilateral activation of the sensorimotor cortex [49, 50].

The term PHS was recently coined by Armstrong-Wells et al. [51] and appeared to include term infants with parenchymal haemorrhage due to different underlying problems. They found a population prevalence of 6.2 in

**Fig. 6** Born at 37 weeks, following antenatal diagnosis of foetal supraventricular tachycardia. MRI, T<sub>2</sub>SE (TR 6284/TE 120) performed on day 3, shows a large left-sided middle cerebral artery infarct of antenatal onset, with evidence of Wallerian degeneration and presence of cysts within the area of infarction. Diffusion tensor tractography shows loss of fibres with the corticospinal tract of the affected hemisphere



100,000 live births. All infants presented with encephalopathy and more than half (65%) with seizures. Perinatal haemorrhagic stroke was typically unifocal (74%) and unilateral (83%). Etiologies included thrombocytopenia ( $n=4$ ) and cavernous malformation ( $n=1$ ); 15 (75%) were idiopathic. Foetal distress and postmaturity were found to be independent predictors. While some of the larger lesions will be recognised with ultrasound, MRI will provide more detailed information, and early DWI will be able to show associated areas with restricted diffusion.

*Cerebral sinovenous thrombosis* (CSVT) occurs in 0.41 per 100,000 liveborn infants [52]. This diagnosis should especially be considered in infants who present without a history of perinatal asphyxia but with seizures and/or lethargy, sometimes in the context of infection or dehydration. Wu et al. [53] first pointed out that CSVT should always be considered in the presence of an intraventricular haemorrhage (IVH), especially when associated with a unilateral thalamic haemorrhage. Thirty-one percent of 29 infants born >36 weeks gestation, who were diagnosed with CSVT, presented with an IVH. Thalamic haemorrhage was diagnosed in 16% of infants with CSVT [53, 54].

Cranial ultrasound may detect CSVT, particularly in the presence of a midline thrombus in the superior sagittal sinus, or a unilateral thalamic haemorrhage. Power Doppler may be superior to colour Doppler when available [55, 56]. Additional imaging is required to exclude CSVT in more peripheral locations and to confirm the extent of the thrombus. Unenhanced CT may detect a thrombus and contrast-enhanced CT may show the ‘empty delta’ sign which is a filling defect in the posterior portion of the superior sagittal sinus due to thrombus. There are false positives and missed diagnoses in up to 40% of children with CSVT [57]. MRI and MR venography or CT venography are needed to confirm the diagnosis [58]. Susceptibility weighted imaging has recently been reported as another useful sequence in confirming the presence of CSVT and following for progression or resolution [59, 60].

## MRS

The technique of MRS enables us to detect different molecules in tissue. Nuclei that have been used clinically for MRS are  $^{31}\text{P}$  and  $^1\text{H}$ . Thereby, *in vivo* brain metabolism can be assessed, and changes can be documented. MRS has been used to study changes in cerebral metabolism of neonates following (perinatal) hypoxia–ischaemia.

### $^{31}\text{P}$ -MRS

$^{31}\text{P}$ -MRS was one of the first MRS techniques to be used in neonates more than two decades ago [6, 7]. With this

technique, metabolites such as high-energy phosphates (phosphocreatine (PCr), nucleotide triphosphates (NTP)) and inorganic phosphate ( $\text{P}_i$ ), phosphomonoesters and phosphodiester can be detected. It is time-consuming to measure absolute concentrations, and therefore, metabolite ratios have been calculated used instead to demonstrate changes in the brain. In addition, intracellular pH can be calculated using the formula published by Petroff et al. [61].

It has been shown that these metabolite ratios change during development, especially during the first years of life [62]. In animal experiments hypoxia decreased PCr/ $\text{P}_i$  and NTP/total phosphate ratios [63]. Full-term neonates with perinatal asphyxia have also been studied [64, 65]. After a successful resuscitation, brain energy metabolism returned to normal to become abnormal after 6–12 h to decrease even further after 24–48 h [65–67]. This coincided with clinical deterioration such as the development of seizures. The concept of ‘secondary energy failure’ has been elaborated in animal models, in particular in newborn piglets [68–70]. Using  $^{31}\text{P}$ -MRS in these animal models, neuroprotective strategies like hypothermia or 2-iminobiotin could be tested [71, 72].

An example of the changes in  $^{31}\text{P}$ -MRS during cerebral hypoxia–ischaemia in the newborn piglet is presented in (Fig. 7). With the increasing experience in human neonates,  $^{31}\text{P}$ -MRS was found to correlate with long-term neurodevelopmental outcome, especially when performed during the first few weeks after the insult [66, 67]. In neonates with a very poor outcome, elevated intracellular pH, the so-called pH paradox, existed even for weeks after the insult, possibly due to changes in the  $\text{Na}^+/\text{H}^+$  transporter.

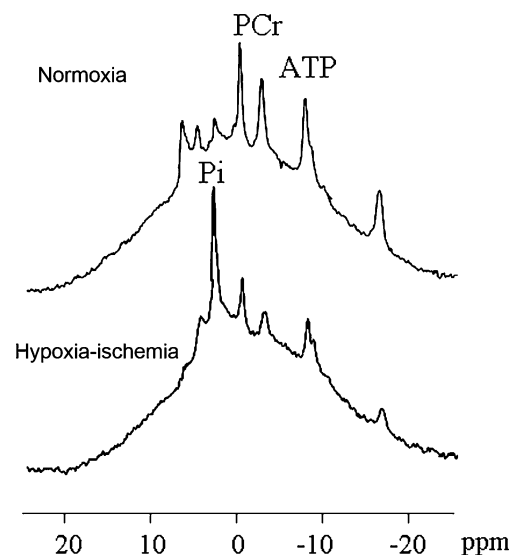


**Fig. 7**  $^{31}\text{P}$ -MRS of a newborn piglet at baseline (*top*) and after 1 h of cerebral hypoxia–ischaemia (*bottom*). The PCr/ $\text{P}_i$  ratio and ATP peaks decreased, whereas the distance between PCr and  $\text{P}_i$  decreased, indicating a decrease in the intracellular pH [14]

Unfortunately, with the magnetic field strength of the current clinical systems, it is impossible to perform localised  $^{31}\text{P}$ -MRS, so only relatively large brain areas can be examined. Due to these limitations,  $^{31}\text{P}$ -MRS has not become a routine clinical tool to assess asphyxiated full-term neonates.

### $^1\text{H}$ -MRS

Proton MRS has also been used in neonates since the early 1990s [62, 73]. Metabolites that can be demonstrated with  $^1\text{H}$ -MRS and echo times of 136 or more milliseconds are choline (Cho), creatine and phosphocreatine as a single peak (Cr), *N*-acetylaspartate (NAA) and—when present—lactate (Lac). With shorter echo times, myo-inositol and the combined glutamate–glutamine–GABA peak can be measured. Given the large amounts of water in the neonatal brain, high-quality water suppression is essential for  $^1\text{H}$ -MRS. The detection level of the aforementioned metabolites is in the millimolar range. As with  $^{31}\text{P}$ -MRS,

providing absolute concentrations of metabolites is difficult, needing internal or external standards. Although some have used water as an internal standard, this may not be appropriate in asphyxiated full-term neonates with changing amounts of intracellular and extracellular brain water [74].

Therefore, metabolite ratios such as NAA/Cho, NAA/Cr or Lac/NAA are used instead [75]. NAA is found mainly in neurons and oligodendroglial precursors. It has been used as a marker of neuronal integrity. With selective loss of neurons, the NAA/Cho ratio will decrease (Fig. 8).

Previously, the changes in  $^1\text{H}$ -MRS during normal development have been demonstrated [62]. In a previous study, we have shown an increase in the NAA/Cho ratio between preterm at a gestational age of 32 weeks and term equivalent age [76]. Others have shown that lactate is a normal component in the preterm brain [77]. We have demonstrated lactate in the brain of the asphyxiated full-term neonate days after the insult [75]. Others have shown that this may persist even for weeks [78]. Experimental work in animals showed accumulation of lactate in the brain during

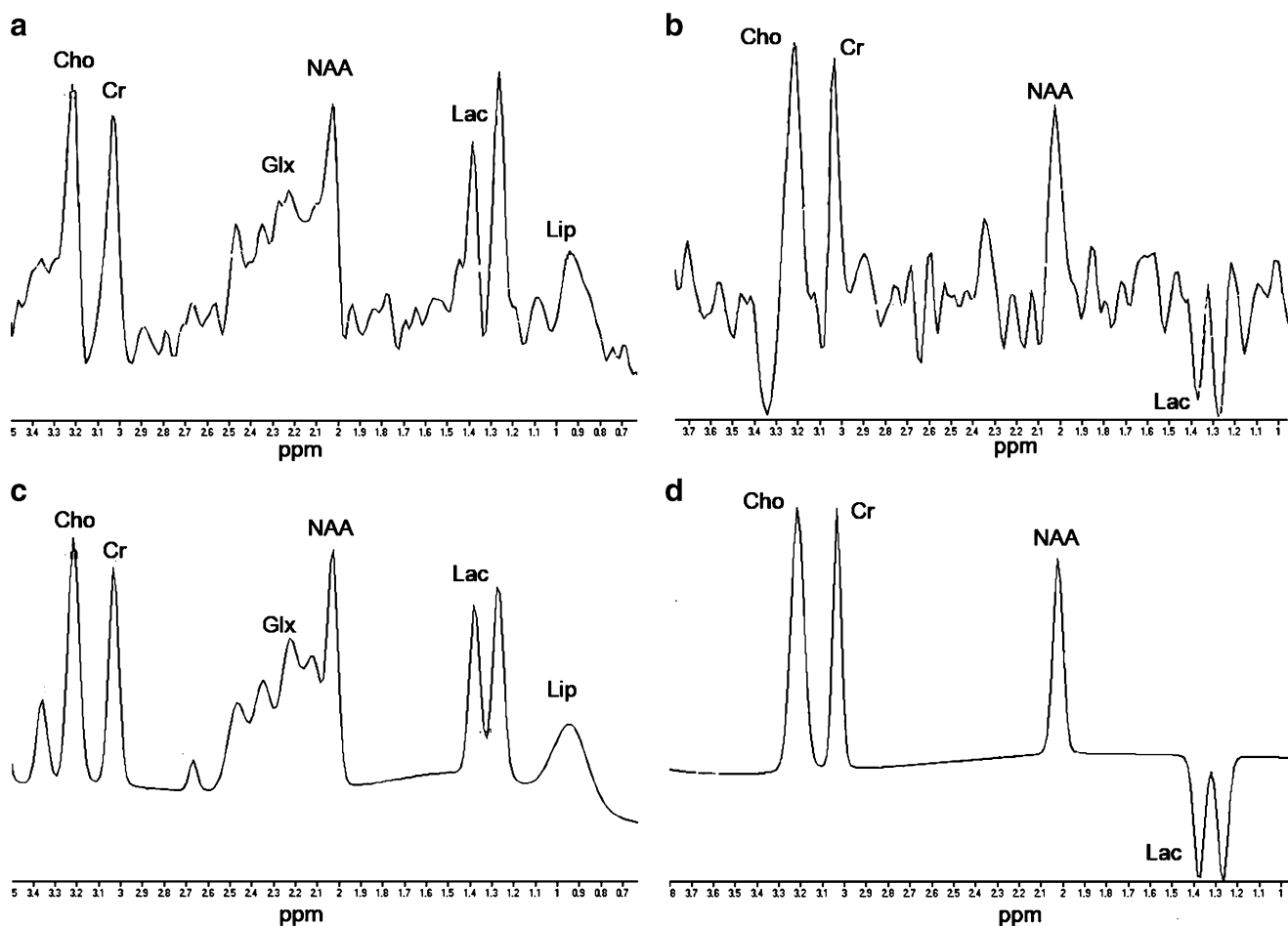


**Fig. 8**  $^1\text{H}$ -MRS of a full-term neonate, 4 days after perinatal asphyxia. NAA/Cho is still within the normal range for full-term neonates, but a very large lactate resonance can be identified at

1.33 ppm. **a** Original spectrum of TE 35 ms, **b** original spectrum of TE 144 ms, **c** fitted spectrum of TE 35 ms, and **d** fitted spectrum of TE 144 ms



secondary energy failure which could be decreased with appropriate neuroprotective strategies [71].

An advantage of  $^1\text{H}$ -MRS over  $^{31}\text{P}$ -MRS is the possibility to perform localised examinations. Volumes of brain tissue as small as 1 cc can be assessed in 1.5-T MR systems. Thereby, changes in brain areas that are particularly vulnerable, such as the basal ganglia and thalamus, can be demonstrated.

In addition, chemical shift imaging enables us to measure metabolites in a matrix of voxels overlying the brain. Thereby, localised elevations of lactate can be demonstrated [79]. An example of this is given in Fig. 9, where  $^1\text{H}$ -MRS chemical shift imaging is presented of a neonate with a large infarct in the territory of the right middle cerebral artery.

One of the limitations of  $^1\text{H}$ -MRS is the loss of quality by susceptibility. Thereby, it is impossible to examine the cortex reliably.

We and others have shown decreases in NAA/Cho or NAA/Cr and elevations of Lac/NAA to predict a poor neurodevelopmental outcome [75, 80]. These studies have recently been summarised [81]. The timing of  $^1\text{H}$ -MRS is less critical than of  $^{31}\text{P}$ -MRS. Measurements performed after the second week of life may show normalised PCr/ $\text{P}_i$  ratios. MR imaging performed before the fourth day after the insult

may not yet demonstrate changes on T1- and T2-weighted images. Diffusion-weighted images may show pseudo-normalisation, which complicates assessment of the severity of the insult. Abnormalities using  $^1\text{H}$ -MRS may only be missed, when this technique is performed very early, i.e. during the first day of life, before the development of secondary energy failure [82].

Based on these aspects, it has been suggested that  $^1\text{H}$ -MRS is the best MR biomarker to predict neurodevelopmental outcome in asphyxiated full-term neonates [81]. However, since brain metabolite ratios may vary between MR systems and coils, development of normal values in one's own setting is required, and support of physicists is mandatory. The limiting factor in the development of these normal values may be the lack of 'normal' neonates who will undergo MR examinations.

## Conclusion

Overall, there has been tremendous progress in the MRI technique over the last few decades. Both MRI and proton MRS can help in detecting different patterns of brain injury in (full-term) human neonates following hypoxic–ischaemic

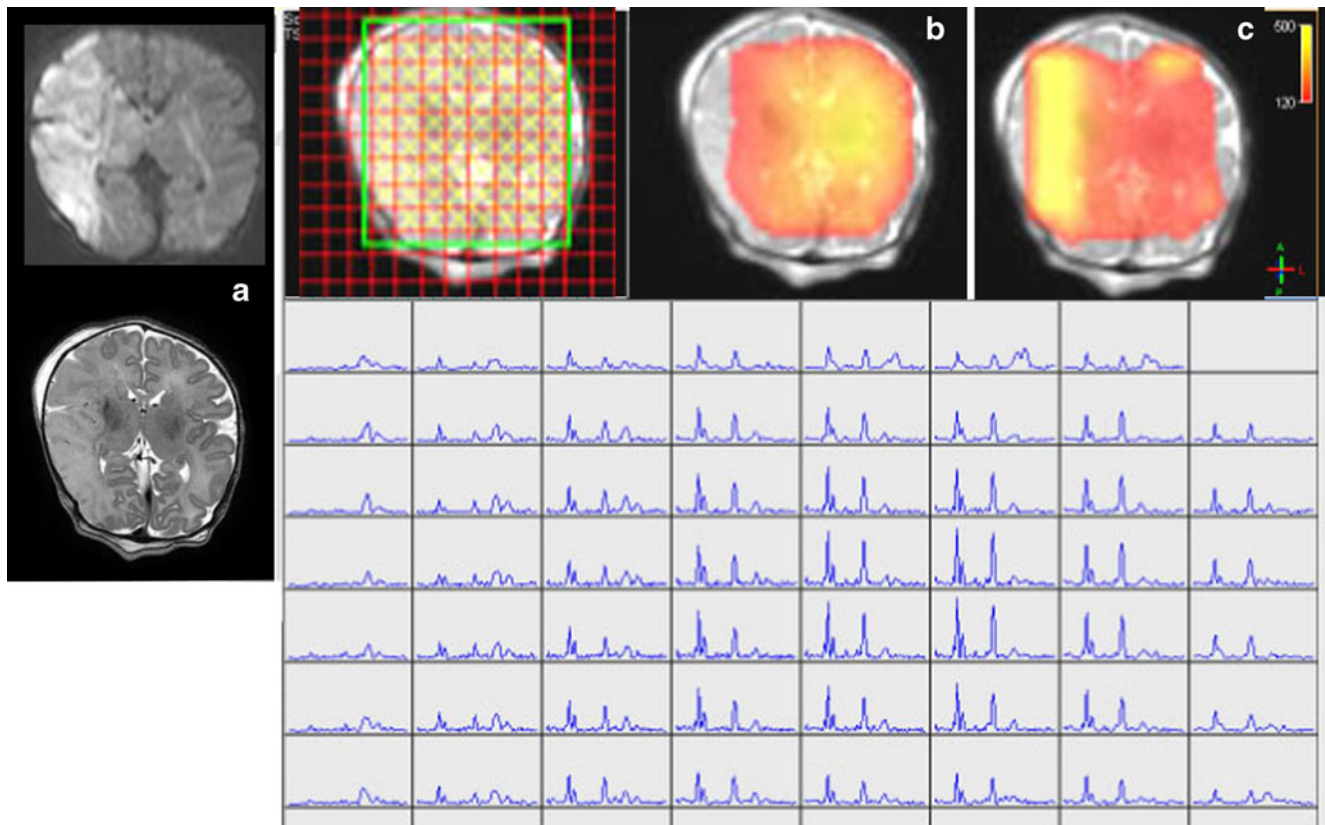


**Fig. 9** Chemical shift imaging a neonate with a large stroke in the territory of the right middle cerebral artery (a). In the infarcted area, NAA concentration is decreased (b, red), whereas Lac/NAA ratio is increased (c, yellow)

brain injury and are extremely useful in predicting neurodevelopmental outcome. We recommend to perform MRI and MRS in every full-term infant with encephalopathy and/or seizures admitted to a neonatal intensive care unit.

**Acknowledgement** The authors would like to thank the technicians and radiologists of the department of radiology for their help.

**Conflict of interest statement** We declare that we have no conflict of interest.

**Open Access** This article is distributed under the terms of the Creative Commons Attribution Noncommercial License which permits any noncommercial use, distribution, and reproduction in any medium, provided the original author(s) and source are credited.

## References

- Ranck JB, Windle WF (1959) Brain damage in the monkey, *Macaca mulatta*, by asphyxia neonatorum. *Exp Neurol* 1:130–154
- Myers RE (1997) Two patterns of perinatal brain damage and their conditions of occurrence. *Am J Obstet Gynecol* 112:246–276
- Okerefor A, Allsop J, Counsell SJ, Fitzpatrick J, Azzopardi D, Rutherford MA, Cowan FM (2008) Patterns of brain injury in neonates exposed to perinatal sentinel events. *Pediatrics* 121:906–914
- Miller SP, Ramaswamy V, Michelson D, Barkovich AJ, Holshouser B, Wycliffe N et al (2005) Patterns of brain injury in term neonatal encephalopathy. *J Pediatr* 146:453–460
- Triulzi F, Parazzini C, Righini A (2006) Patterns of damage in the mature neonatal brain. *Pediatr Radiol* 36:608–620
- Cady EB, Costello AM, Dawson MJ, Delpy DT, Hope PL, Reynolds EO et al (1983) Non-invasive investigation of cerebral metabolism in newborn infants by phosphorus nuclear magnetic resonance spectroscopy. *Lancet* 1:1059–1062
- Younkin DP, Delivoria-Papadopoulos M, Leonard JC, Subramanian VH, Eleff S, Leigh JS Jr et al (1984) Unique aspects of human newborn cerebral metabolism evaluated with phosphorus nuclear magnetic resonance spectroscopy. *Ann Neurol* 16:581–586
- Daneman A, Epelman M, Blaser S, Jarrin JR (2006) Imaging of the brain in full-term neonates: does sonography still play a role? *Pediatr Radiol* 36:636–646
- Ment LR, Bada HS, Barnes P, Grant PE, Hirtz D, Papile LA et al (2002) Practice parameter: neuroimaging of the neonate: report of the Quality Standards Subcommittee of the American Academy of Neurology and the Practice Committee of the Child Neurology Society. *Neurology* 58:1726–1738
- Perrin RG, Rutka JT, Drake JM, Meltzer H, Hellman J, Jay V et al (1997) Management and outcomes of posterior fossa subdural hematomas in neonates. *Neurosurgery* 40:1190–1199, discussion 1199–200
- Brouwer AJ, Groenendaal F, Koopman C, Nieuvelstein RJ, Han KS, de Vries LS. Intracranial hemorrhage in full-term newborns: a hospital-based cohort study. *Neuroradiology* (in press)
- Pasternak JF, Gorey MT (1998) The syndrome of acute near-total intrauterine asphyxia in the term infant. *Pediatr Neurol* 18:391–398
- Cowan F, Rutherford M, Groenendaal F, Eken P, Mercuri E, Bydder GM et al (2003) Origin and timing of brain lesions in term infants with neonatal encephalopathy. *Lancet* 361:736–742
- Leijser LM, de Vries LS, Rutherford MA, Manzur AY, Groenendaal F, de Koning TJ et al (2007) Cranial ultrasound in metabolic disorders presenting in the neonatal period: characteristic features and comparison with MR imaging. *AJNR Am J Neuroradiol* 28:1223–1231
- McKinstry RC, Miller JH, Snyder AZ, Mathur A, Scheff GL, Almlil CR et al (2002) A prospective, longitudinal diffusion tensor imaging study of brain injury in newborns. *Neurology* 24(59):824–833
- Liauw L, van Wezel-Meijler G, Veen S, van Buchem MA, van der Grond J (2009) Do apparent diffusion coefficient measurements predict outcome in children with neonatal hypoxic–ischemic encephalopathy? *AJNR Am J Neuroradiol* 30:264–270
- Malik GK, Trivedi R, Gupta RK, Hasan KM, Hasan M, Gupta A et al (2006) Serial quantitative diffusion tensor MRI of the term neonates with hypoxic–ischemic encephalopathy (HIE). *Neuropediatrics* 37:337–343
- Soul JS, Robertson RL, Tzika AA, du Plessis AJ, Volpe JJ (2001) Time course of changes in diffusion-weighted magnetic resonance imaging in a case of neonatal encephalopathy with defined onset and duration of hypoxic–ischemic insult. *Pediatrics* 108:1211–1214
- Barkovich AJ, Miller SP, Bartha A, Newton N, Hamrick SE, Mukherjee P et al (2006) MR imaging, MR spectroscopy, and diffusion tensor imaging of sequential studies in neonates with encephalopathy. *AJNR Am J Neuroradiol* 27:533–547
- Perlman JM (2003) Intrapartum asphyxia and cerebral palsy: is there a link? *Clin Perinatol* 33:335–353
- Rutherford MA, Pennock JM, Counsell SJ, Mercuri E, Cowan FM, Dubowitz LM et al (1998) Abnormal magnetic resonance signal in the internal capsule predicts poor neurodevelopmental outcome in infants with hypoxic–ischemic encephalopathy. *Pediatrics* 102:323–328
- Rutherford M, Counsell S, Allsop J, Boardman J, Kapellou O, Larkman D et al (2004) Diffusion-weighted magnetic resonance imaging in term perinatal brain injury: a comparison with site of lesion and time from birth. *Pediatrics* 114:1004–1014
- Hunt RW, Neil JJ, Coleman LT, Kean MJ, Inder TE (2004) Apparent diffusion coefficient in the posterior limb of the internal capsule predicts outcome after perinatal asphyxia. *Pediatrics* 114:999–1003
- Ward P, Counsell S, Allsop J, Cowan F, Shen Y, Edwards D, Rutherford M (2006) Reduced fractional anisotropy on diffusion tensor magnetic resonance imaging after hypoxic–ischemic encephalopathy. *Pediatrics* 117:e619–e630
- Himmelman K, Hagberg G, Wiklund LM, Eek MN, Uvebrant P (2007) Dyskinetic cerebral palsy: a population-based study of children born between 1991 and 1998. *Dev Med Child Neurol* 49:246–251
- Groenendaal F, de Vries LS (2005) Watershed infarcts in the full term neonatal brain. *Arch Dis Child Fetal Neonatal Ed* 90:F488
- Chau V, Poskitt KJ, Sargent MA, Lupton BA, Hill A, Roland E, Miller SP (2009) Comparison of computer tomography and magnetic resonance imaging scans on the third day of life in term newborns with neonatal encephalopathy. *Pediatrics* 123:319–326
- Rutherford M, Pennock J, Schwieso J, Cowan F, Dubowitz L (1996) Hypoxic–ischemic encephalopathy: early and late magnetic resonance imaging findings in relation to outcome. *Arch Dis Child Fetal Neonatal Ed* 75:F145–F151
- Burns C, Boardman J, Rutherford M et al (2008) Patterns of cerebral injury and neurodevelopmental outcome following symptomatic neonatal hypoglycaemia. *Pediatrics* 122:65–74
- Sato Y, Hayakawa M, Iwata O, Okumura A, Kato T, Hayakawa F et al (2008) Delayed neurological signs following isolated parasagittal injury in asphyxia at term. *Eur J Paediatr Neurol* 12:359–365
- Mercuri E, Ricci D, Cowan FM, Lessing D, Frisone MF, Haataja L et al (2000) Head growth in infants with hypoxic–ischemic

- encephalopathy: correlation with neonatal magnetic resonance imaging. *Pediatrics* 106:235–243
32. Steinman KJ, Gorno-Tempini ML, Glidden DV, Kramer JH, Miller SP, Barkovich AJ, Ferriero DM (2009) Neonatal watershed brain injury on magnetic resonance imaging correlates with verbal IQ at 4 years. *Pediatrics* 123:1025–1030
  33. Miller SP, Ferriero NN, DM PJC, Glidden DV, Barnwell A et al (2002) Predictors of 30-month outcome after perinatal depression: role of proton MRS and socioeconomic factors. *Pediatr Res* 52:71–77
  34. Oguni H, Sugama M, Osawa M (2008) Symptomatic parieto-occipital epilepsy as sequela of perinatal asphyxia. *Pediatr Neurol* 38:345–352
  35. Vermeulen RJ, Fetter WP, Hendriks L, Van Schie PE, van der Knaap MS, Barkhof F (2003) Diffusion-weighted MRI in severe neonatal hypoxic ischaemia: the white cerebrum. *Neuropediatrics* 34:72–76
  36. Dodelson DK, Grosso C (2005) Maternal mutation 677C>T in the ethylenetetrahydrofolate reductase gene associated with severe brain injury in offspring. *Clin Genet* 67:69–80
  37. Li AM, Chau V, Poskitt KJ, Sargent MA, Lupton BA, Hill A et al (2009) White matter injury in term newborns with neonatal encephalopathy. *Pediatr Res* 65:85–89
  38. Galli KK, Zimmerman RA, Jarvik GP, Wernovsky G, Kuypers MK, Clancy RR et al (2004) Periventricular leukomalacia is common after neonatal cardiac surgery. *J Thorac Cardiovasc Surg* 127:692–704
  39. Ramaswamy V, Miller SP, Barkovich AJ, Partridge JC, Ferriero DM (2004) Perinatal stroke in term infants with neonatal encephalopathy. *Neurology* 62:2088–2091
  40. Cheong JL, Cowan FM (2009) Neonatal arterial ischaemic stroke: obstetric issues. *Semin Fetal Neonatal Med* 14:267–271
  41. Cowan F, Mercuri E, Groenendaal F, Bassi L, Ricci D, Rutherford M, de Vries LS (2005) Does cranial ultrasound imaging identify arterial cerebral infarction in term neonates? *Arch Dis Child Fetal Neonatal Ed* 90:F252–F256
  42. De Vries LS, Van der Grond J, Van Haastert IC, Groenendaal F (2005) Prediction of outcome in new-born infants with arterial ischaemic stroke using diffusion-weighted magnetic resonance imaging. *Neuropediatrics* 36:12–20
  43. Kirton A, Shroff M, Visvanathan T, deVeber G (2007) Quantified corticospinal tract diffusion restriction predicts neonatal stroke outcome. *Stroke* 38:974–980
  44. Lequin MH, Dudink J, Tong KA, Obenaus A (2009) Magnetic resonance imaging in neonatal stroke. *Semin Fetal Neonatal Med* 14:299–310
  45. Glenn OA, Ludeman NA, Berman JI, Wu YW, Lu Y, Bartha AI et al (2007) Diffusion tensor MR imaging tractography of the pyramidal tracts correlates with clinical motor function in children with congenital hemiparesis. *AJNR Am J Neuroradiol* 28:1796–1802
  46. Ashwal S, Obenaus A, Snyder EY (2009) Neuroimaging as a basis for rational stem cell therapy. *Pediatr Neurol* 40:227–236
  47. Staudt M, Grodd W, Gerloff C, Erb M, Stitz J, Krägeloh-Mann I (2002) Two types of ipsilateral reorganization in congenital hemiparesis: a TMS and fMRI study. *Brain* 125:2222–2237
  48. Seghier ML, Lazeyras F, Zimine S, Saudan-Frei S, Safran AB, Huppi PS (2005) Visual recovery after perinatal stroke evidenced by functional and diffusion MRI: case report. *BMC Neurol* 26(5):17
  49. Arichi T, Moraux A, Melendez A, Doria V, Groppo M, Merchant N et al (2009) Somatosensory cortical activation identified by functional MRI in preterm and term infants. *Neuroimage* 49(3):2063–2071
  50. Heep A, Scheef L, Jankowski J, Born M, Zimmermann N, Sival D et al (2009) Functional magnetic resonance imaging of the sensorimotor system in preterm infants. *Pediatrics* 123:294–300
  51. Armstrong-Wells J, Johnston SC, Wu YW, Sidney S, Fullerton HJ (2009) Prevalence and predictors of perinatal hemorrhagic stroke: results from the Kaiser Pediatric Stroke Study. *Pediatrics* 123:823–828
  52. deVeber G, Andrew M, Adams C, Bjornson B, Booth F, Buckley DJ et al (2001) Cerebral sinovenous thrombosis in children. *N Engl J Med* 345:417–423
  53. Wu YW, Miller SP, Chin K, Collins AE, Lomeli SC, Chuang NA et al (2002) Multiple risk factors in neonatal sinovenous thrombosis. *Neurology* 59:438–440
  54. Kersbergen KJ, de Vries LS, van Straaten HL, Benders MJ, Nievelstein RA, Groenendaal F (2009) Anticoagulation therapy and imaging in neonates with a unilateral thalamic hemorrhage due to cerebral sinovenous thrombosis. *Stroke* 40:2754–2760
  55. Govaert P, Voet D, Achten E, Vanhaesebrouck P, van Rostenberghe H, van Gysel D et al (1992) Noninvasive diagnosis of superior sagittal sinus thrombosis in a neonate. *Am J Perinatol* 9:201–204
  56. Tsao PN, Lee WT, Peng SF, Lin JH, Yau KI (1999) Power Doppler ultrasound imaging in neonatal cerebral venous sinus thrombosis. *Pediatr Neurol* 21:652–655
  57. Davies RP, Slavotinek JP (1994) Incidence of the empty delta sign in computed tomography in the paediatric age group. *Australas Radiol* 38:17–19
  58. Eichler F, Krishnamoorthy K, Grant PE (2007) Magnetic resonance imaging evaluation of possible neonatal sinovenous thrombosis. *Pediatr Neurol* 37:317–323
  59. Takekawa H, Tanaka H, Ogawa T, Nijjima Y, Sada T, Daimon Y et al (2008) Usefulness of echo-planar T2\* susceptibility-weighted imaging for reliable diagnosis of cerebral venous sinus thrombosis. *Intern Med* 47:2101–2102
  60. Kawabori M, Kuroda S, Kudo K, Terae S, Kaneda M, Nakayama N et al (2009) Susceptibility-weighted magnetic resonance imaging detects impaired cerebral hemodynamics in the superior sagittal sinus thrombosis—case report. *Neurol Med Chir (Tokyo)* 49:248–251
  61. Petroff OA, Prichard JW, Behar KL, Rothman DL, Alger JR, Shulman RG (1985) Cerebral intracellular pH by <sup>31</sup>P nuclear magnetic resonance spectroscopy. *Neurology* 35:781–788
  62. van der Knaap MS, van der Grond J, van Rijen PC, Faber JA, Valk J, Willemsse K (1990) Age-dependent changes in localized proton and phosphorus MR spectroscopy of the brain. *Radiology* 176:509–515
  63. Younkun DP, Wagerle LC, Chance B, Maria J, Delivoria-Papadopoulou M (1987) <sup>31</sup>P-NMR studies of cerebral metabolic changes during graded hypoxia in newborn lambs. *J Appl Physiol* 62:1569–1574
  64. Hope PL, Costello AM, Cady EB, Delpy DT, Tofts PS, Chu A et al (1984) Cerebral energy metabolism studied with phosphorous NMR spectroscopy in normal and birth asphyxiated infants. *Lancet* 8399:366–370
  65. Wyatt JS, Edwards AD, Azzopardi D, Reynolds EO (1989) Magnetic resonance and near infrared spectroscopy for investigation of perinatal hypoxic–ischaemic brain injury. *Arch Dis Child* 64:953–963
  66. Moorcraft J, Bolas NM, Ives NK, Ouwerkerk R, Smyth J, Rajagopalan B et al (1991) Global and depth resolved phosphorus magnetic resonance spectroscopy to predict outcome after birth asphyxia. *Arch Dis Child* 66:1119–1123
  67. Roth SC, Edwards AD, Cady EB, Delpy DT, Wyatt JS, Azzopardi D et al (1992) Relation between cerebral oxidative metabolism following birth asphyxia, and neurodevelopmental outcome and brain growth at one year. *Dev Med Child Neurol* 34:285–295
  68. Lorek A, Takei Y, Cady EB, Wyatt JS, Penrice J, Edwards AD et al (1994) Delayed (“secondary”) cerebral energy failure after acute hypoxia-ischemia in the newborn piglet: continuous 48-hour

- studies by phosphorus magnetic resonance spectroscopy. *Pediatr Res* 36:699–706
69. Penrice J, Lorek A, Cady EB, Amess PN, Wylezinska M, Cooper CE et al (1997) Proton magnetic resonance spectroscopy of the brain during acute hypoxia–ischemia and delayed cerebral energy failure in the newborn piglet. *Pediatr Res* 41:795–802
70. Groenendaal F, de Graaf RA, van Vliet G, Nicolay K (1999) Effects of hypoxia–ischemia and inhibition of nitric oxide synthase on cerebral energy metabolism in newborn piglets. *Pediatr Res* 45:827–833
71. Amess PN, Penrice J, Cady EB, Lorek A, Wylezinska M, Cooper CE et al (1997) Mild hypothermia after severe transient hypoxia–ischemia reduces the delayed rise in cerebral lactate in the newborn piglet. *Pediatr Res* 41:803–808
72. Peeters-Scholte C, Koster JG, Veldhuis W, van den Tweel E, Zhu C, Kops N et al (2002) Neuroprotection by selective nitric oxide synthase inhibition at 24 hours after perinatal hypoxia–ischemia. *Stroke* 33:2304–2310
73. Peden CJ, Cowan FM, Bryant DJ, Sargentoni J, Cox JJ, Menon DK et al (1990) Proton MR spectroscopy of the brain in infants. *J Comput Assist Tomogr* 14:886–894
74. Toft PB, Leth H, Lou H, Pryds O, Henriksen O (1994) Metabolite concentrations in the developing brain estimated with proton MR spectroscopy. *J Magn Reson Imaging* 4:674–680
75. Groenendaal F, Veenhoven RH, van der Grond J, Jansen GH, Witkamp TD, de Vries LS (1994) Cerebral lactate and N-acetyl-aspartate/choline ratios in asphyxiated full-term neonates demonstrated in vivo using proton magnetic resonance spectroscopy. *Pediatr Res* 35:148–151
76. Roelants-van Rijn AM, van der Grond J, Stigter RH, de Vries LS, Groenendaal F (2004) Cerebral structure and metabolism, and long-term outcome in small-for-gestational-age preterm neonates. *Pediatr Res* 56:285–290
77. Leth H, Toft PB, Pryds O, Peitersen B, Lou HC, Henriksen O (1995) Brain lactate in preterm and growth-retarded neonates. *Acta Paediatr* 84:495–499
78. Robertson NJ, Cox JJ, Cowan FM, Counsell SJ, Azzopardi D, Edwards AD (1999) Cerebral intracellular lactic acidosis persisting months after neonatal encephalopathy measured by magnetic resonance spectroscopy. *Pediatr Res* 46:287–296
79. Groenendaal F, van der Grond J, Witkamp TD, de Vries LS (1995) Proton magnetic resonance spectroscopic imaging in neonatal stroke. *Neuropediatrics* 26:243–248
80. Roelants-van Rijn AM, van der Grond J, de Vries LS, Groenendaal F (2001) Value of  $^1\text{H}$ -MRS using different echo times in neonates with cerebral hypoxia–ischemia. *Pediatr Res* 49:356–362
81. Thayyil S, Chandrasekaran M, Taylor A, Bainbridge A, Cady EB, Chong WK et al (2010) Cerebral magnetic resonance biomarkers in neonatal encephalopathy: a meta-analysis. *Pediatrics* 125:e382–e395
82. L'Abée C, de Vries LS, van der Grond J, Groenendaal F (2005) Early diffusion-weighted MRI and  $^1\text{H}$ -magnetic resonance spectroscopy in asphyxiated full-term neonates. *Biol Neonate* 88:306–312